Simplified design of nonlinear energy sinks for MDOF structures excited by white noise base excitations

AIMETA 2017
XXIII Conference
The Italian Association of Theoretical and Applied Mechanics
Luigi Ascione, Valentino Berardi, Luciano Feo, Fernando Fraternali and Antonio Michele Tralli (eds.)
Salerno, Italy, 4–7 September 2017

SIMPLIFIED DESIGN OF NONLINEAR ENERGY SINKS FOR MDOF STRUCTURES EXCITED BY WHITE NOISE BASE EXCITATIONS

Maria Oliva[1], Giorgio Barone[2], Francesco Lo Iacono[1] and Giacomo Navarra[1]

[1]Facoltà di Ingegneria ed Architettura, Università degli Studi di Enna "Kore"
Cittadella Universitaria, 94100 Enna, Italy
e-mail: {maria.oliva, francesco.loiacono, giacomo.navarra}@unikore.it

[2] School of Architecture, Building and Civil Engineering, Loughborough University
Loughborough, Leicestershire, UK
e-mail: g.barone@lboro.ac.uk

Keywords: Nonlinear Energy Sinks, performance analysis, white noise.

Abstract. *Passive control devices are often used to protect slender and flexible structures from dynamic actions, including earthquakes, wind and waves. The Nonlinear Energy Sink (NES) has recently received increasing attention from researchers because of its capability to passively and irreversibly absorb a significant amount of energy from the primary system over a wide range of frequencies. In this paper, the application of two NESs acting in orthogonal directions is considered to mitigate the response of a multi degree of freedom structure. Parameters for each NES are obtained by considering a single degree of freedom structure, whose mass and frequency are designed based on the fundamental mode of the original structure along the direction of action of the device, and applying the empirical expressions proposed in Oliva et al. (2017). Compared to standard Monte Carlo simulations, the use of these expressions requires a significant lower computational effort, making their implementation suitable for practical engineering purposes. A numerical application on a three-dimensional building is presented to demonstrate the effectiveness of the proposed method. The NESs performance is analysed varying the direction of the ground motion, showing the potential of this passive control system in civil engineering applications. Results are reported in terms of statistics of the structural response, determined by Monte Carlo simulation, and analysis of the energy dissipated by the control devices.*

1 INTRODUCTION

In the last decades, great attention has been paid to research and to develop structural control systems capable of protecting slender and flexible structures from dynamic actions. Passive devices have been widely used for civil engineering structures because they require no external power source to operate, they are usually relatively inexpensive and inherently stable [1]. However, the most commonly used passive absorbers (i.e.TMDs and TLCDs), have limited control capacity since they are generally tuned to a single structural natural frequency [2–5]. They are effective within a narrow frequency band and are very sensitive to detuning, that could occur as effect of ageing, temperature or humidity variations, etcetera.

An efficient way to overcome these limitations is the use of the Nonlinear Energy Sink (NES), consisting of a small mass coupled to the main structure with an essentially nonlinear spring, which enables the device to resonate with any of the linearised modes of the primary system, and a linear viscous damping element, which dissipates the vibrational energy transferred through resonant modal interactions. NES strong nonlinear nature precludes the existence of preferential resonant frequencies, hence reducing its sensitiveness to detuning. On the other hand, the nonlinear stiffness makes the NES particularly sensitive to loading perturbations. An additional feature of this device is the so-called Targeted Energy Transfer (TET) or Nonlinear Energy Pumping, i.e. the irreversible energy transfer from the primary structure to the NES. TET has been widely investigated by many researchers through perturbations methods, bifurcation and time-frequency analyses [6–12], as well as small and large-scale experimental tests [13–18]. It occurs when the input energy is above a certain critical level and can be activated by one among three mechanisms: fundamental resonance capture, sub-harmonic resonance capture, and nonlinear beating.

Due to its complex dynamic behaviour, the design of the main NES parameters is not straightforward, hence the need for simplified design procedures of easy application for standard structures and excitations. Closed-form solutions to determine the optimal value of the NES nonlinear stiffness capable to trigger TET have been proposed for transient and harmonic excitations in [19–21]. Empirical formulae for determining the optimal parameters of an ungrounded and lightweight NES installed on a Single Degree Of Freedom (SDOF) structure under white noise base excitations have been recently proposed for pre-design purposes in [22], based on the numerical results of a campaign of Monte Carlo Simulations (MCSs) by varying the main structural parameters and the intensity of the external excitation.

In this paper, a simplified design procedure of two NESs acting in orthogonal directions is proposed in order to reduce the dynamic response of MDOF structures subject to white noise base excitations. The authors extend the application of the empirical formulae previously proposed for SDOF structures [22], by considering dummy oscillators whose masses and natural frequencies depend on the effective modal masses and modal frequencies of the main structure. A two-storey steel frame has been used to show the effectiveness of the proposed passive control system, considering several scenarios by varying the direction of the ground motion acting on the structure. Results are reported in terms of statistics of the response and energy dissipated by the control devices.

2 GOVERNING EQUATIONS

Consider a n-DOF linear structure connected to p lightweight NESs through pure cubic stiffnesses and linear viscous dampers, and subject to a white noise ground motion process sample $\ddot{X}_g(t)$. The dynamic equations of motion of the system in its uncontrolled configuration

(i.e. with no NES attached) assume the following form:

$$\mathbf{M}_u\ddot{\mathbf{X}}_u(t) + \mathbf{C}_u\dot{\mathbf{X}}_u(t) + \mathbf{K}_u\mathbf{X}_u(t) = -\mathbf{M}_u\boldsymbol{\tau}_u\ddot{X}_g(t) \tag{1}$$

where $\mathbf{X}_u(t)$, $\dot{\mathbf{X}}_u(t)$, $\ddot{\mathbf{X}}_u(t)$ are the n-dimensional generalised displacement vector and its derivatives, respectively; capital letters indicate stochastic processes; $\boldsymbol{\tau}$ is the influence vector; $\mathbf{M}_u$, $\mathbf{C}_u$ and $\mathbf{K}_u$ are the mass, damping and linear stiffness matrices of the primary system, respectively. On the other hand, in its controlled configuration the dynamic equations become:

$$\mathbf{M}\ddot{\mathbf{X}}(t) + \mathbf{C}\dot{\mathbf{X}}(t) + \mathbf{K}\mathbf{X}(t) + \mathbf{g}(\mathbf{X}(t)) = -\mathbf{M}\boldsymbol{\tau}\ddot{X}_g(t) \tag{2}$$

in which $\mathbf{X}(t)$, $\dot{\mathbf{X}}(t)$, $\ddot{\mathbf{X}}(t)$ are the N-dimensional generalised displacement vector and its derivatives, respectively; $N = n + p$ is the number of degrees of freedom of the combined system; $\mathbf{M}$, $\mathbf{C}$ and $\mathbf{K}$ are the mass, damping and linear stiffness matrices of the combined system, respectively, i.e.:

$$\mathbf{X}(t) = \begin{bmatrix} \mathbf{X}_u \\ \mathbf{X}_{NES} \end{bmatrix} \tag{3}$$

$$\mathbf{M} = \begin{bmatrix} \mathbf{M}_u & \mathbf{0}_{(n\times p)} \\ \mathbf{0}_{(p\times n)} & \mathbf{M}_{NES} \end{bmatrix} \tag{4}$$

$$\mathbf{C} = \begin{bmatrix} \mathbf{C}_u & \mathbf{0}_{(n\times p)} \\ \mathbf{0}_{(p\times n)} & \mathbf{0}_{(p\times p)} \end{bmatrix} + \mathbf{L}\mathbf{C}_{NES}\mathbf{L}^{\mathrm{T}} \tag{5}$$

$$\mathbf{K} = \begin{bmatrix} \mathbf{K}_u & \mathbf{0}_{(n\times p)} \\ \mathbf{0}_{(p\times n)} & \mathbf{0}_{(p\times m)} \end{bmatrix} \tag{6}$$

In Eq. 5, $\mathbf{L}$ is the $N \times p$ linear transformation matrix returning the vector of relative displacements of each NES device, $\mathbf{Y}(t)$, as a function of the selected degrees of freedom:

$$\mathbf{Y}(t) = \mathbf{L}\mathbf{X}(t) \tag{7}$$

with the i-th column of $\mathbf{L}$ corresponding to the i-th NES. Moreover, $\mathbf{M}_{NES}$ and $\mathbf{C}_{NES}$ are the diagonal matrices of mass and the linear damping of the NESs, respectively, whereas $\mathbf{g}(\mathbf{X})$ is the vector collecting all the nonlinear forces. The latter can be expressed, in general, as a function of the relative displacements $\mathbf{Y}$ as:

$$\mathbf{g}(\mathbf{X}) = \mathbf{L}^{\mathrm{T}}\,\mathbf{g}_L(\mathbf{Y}) \tag{8}$$

where the i-th term of the vector $\mathbf{g}_L(\mathbf{Y})$ is:

$$\{\mathbf{g}_L(\mathbf{Y})\}_i = k_{NES,i}\,Y_i^3 \tag{9}$$

being $k_{NES,i}$ the nonlinear stiffness of the i-th NES.

3 SIMPLIFIED DESIGN OF THE NES FOR MDOF STRUCTURES

To the authors' knowledge, there are neither analytical nor numerical formulae for determining the NES parameters for the mitigation of the dynamical response of MDOF structures excited by random excitations. In this section, a simplified procedure is proposed for the case of a single NES aimed at mitigating the vibrations in a pre-determined direction of motion,

selected as reference degree of freedom for the main structure. The same procedure will be extended to the case of two concurrent NESs acting in orthogonal directions into next sections.

The first step in the proposed design approach is the definition of a dummy SDOF oscillator having mass equivalent to the effective modal mass at the first mode of the main structure, $m_{1,e}$, and frequency and damping equivalent to its first modal frequency and damping, $\omega_{1,e}$ and $\zeta_{1,e}$, respectively. The mass ratio between the NES and the dummy structure, $\varepsilon_e = m_{NES}/m_{1,e}$, is assigned based on engineering judgements.

Then, based on [22], the optimal parameters of the NES can be determined as:

$$\begin{aligned} m_{NES} &= \varepsilon_e \cdot m_{1,e} \\ c_{NES} &= \lambda_{opt} \cdot m_{1,e} \\ k_{NES} &= \kappa_{opt} \cdot m_{1,e} \end{aligned} \tag{10}$$

in which:

$$\log_{10} \kappa_{opt} = -\log_{10} S_0 + 4.98 \log_{10} \omega_{1,e} + 0.21 \log_{10} \zeta_{1,e} + 1.33 \log_{10} \varepsilon_e - 1.908 \tag{11}$$

$$\lambda_{opt} = (0.204\, \varepsilon_e - 0.001)\, \zeta_{1,e}^{-0.1} \omega_{1,e} \tag{12}$$

and S_0 is the white noise Power Spectral Density (PSD) amplitude expressed in $(\mathrm{m/s^2})^2/(\mathrm{rad/s})$.

Eqs. (11) and (12) show that:

- κ_{opt} is inversely proportional to the amplitude of the PSD function of the white noise, yet it increases with the frequency $\omega_{1.e}$, damping ratio $\zeta_{1.e}$, and mass ratio ε_e.
- λ_{opt} is independent from the intensity of the white noise excitation, increases for increasing frequency $\omega_{1.e}$ and mass ratio $\varepsilon_{1.e}$ and for decreasing damping ratio of the SDOF equivalent structure, $\zeta_{1.e}$.

Alternatively, based on Eqs. (11) and (12), optimal NES design charts can be considered to determine the optimal NES parameters. These charts allow to quickly determine the optimal NES damping and stiffness for assigned main structure, and selected mass ratio and intensity of the random excitation.

An example of chart is shown in Figure 1, for the case of $\varepsilon_e = 0.05$. The chart reports curves corresponding to various frequencies (black lines) and damping ratios (red lines). Once the exact values for $f_{1,e}$ and $\zeta_{1,e}$ are known, the intersection of matching curves returns the optimal NES damping on the horizontal axis, and the logarithm of the product $(\kappa_{opt}\, S_0)$ on the vertical one (i.e. the optimal nonlinear stiffness is identified once the amplitude of the white noise is determined).

The procedure for determining the optimal NES parameters, proposed in [22], has been tested by means of an error analysis in terms of the reduction of the structural response, and using as performance index the ratio of the Root Mean Square (RMS) of the displacements of a reference structure in its controlled and uncontrolled configurations. Figure 2 reports the variation of the selected performance index with respect to the normalised nonlinear stiffness of the NES, κ, and the normalised NES damping coefficient, λ, and the corresponding value obtained by designing the NES by means of Eqs. (11) and (12) (red dot), showing that the proposed formulae are able to find the optimal parameters with high accuracy and reduced computational effort.

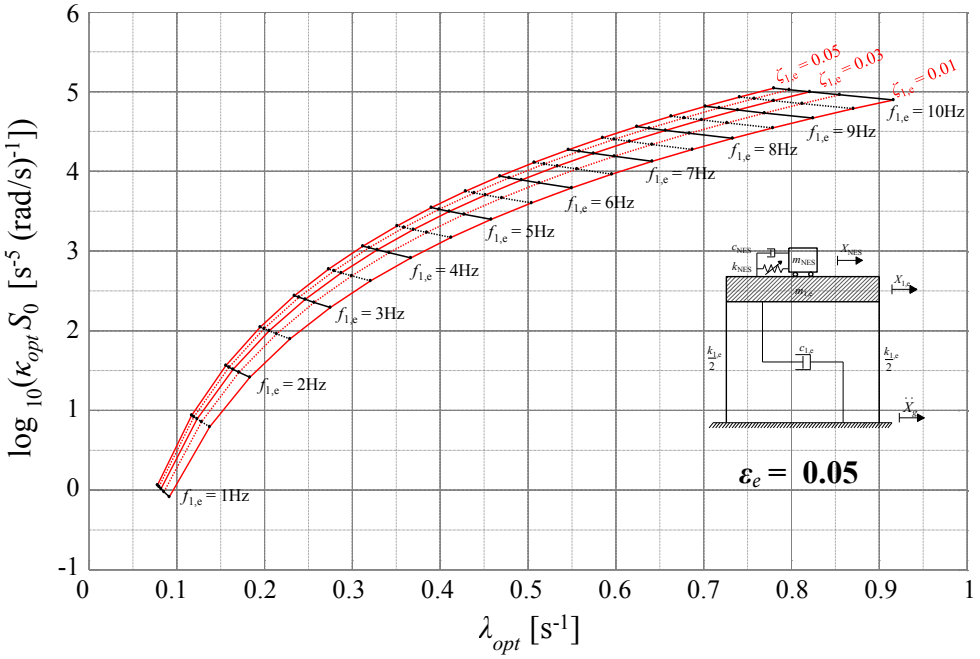

Figure 1: Design chart for determining the optimal NES parameters.

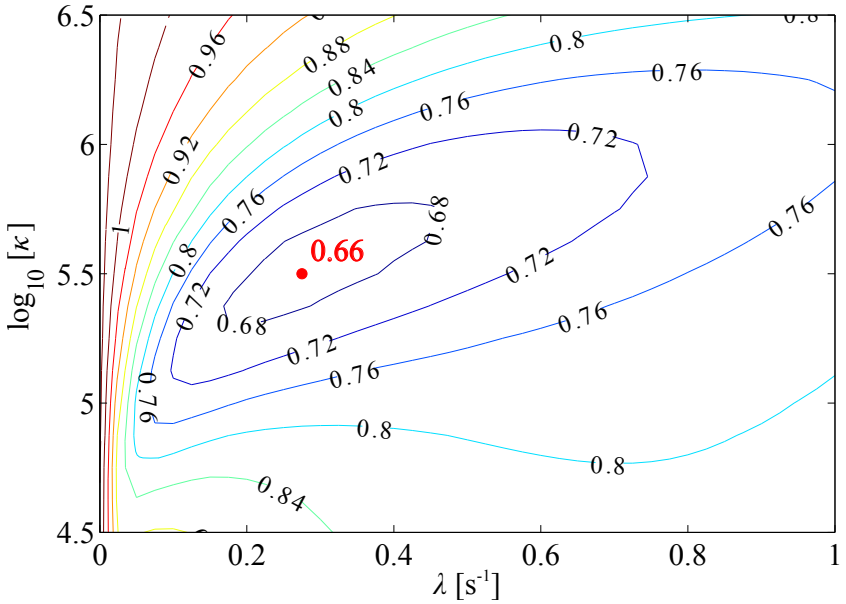

Figure 2: Optimal NES parameters obtained using the empirical formulae on a SDOF reference structure (adapted from [22]).

4 CASE STUDY

The applicability of the proposed optimisation procedure for MDOF structures is herein presented through a numerical application on the low-rise, multi-bay building depicted in Figure 3. The structure is a two-storey steel frame having an overall height of 7.5 m (4 m + 3.5 m) and a mass of approximately 86 tons. The building has two geometrical axes of symmetry, in the following indicated as x and y. However, in order to take into account the uncertainties on

the actual position of the centre of mass (e.g. effects of uneven variable load distributions), the latter has been positioned at a distance equal to 5% of the overall building dimensions, both along the x and y directions. Each floor consists of concrete slabs supported by six HE400A steel columns, and IPE360 beams. A schematic representation of the system is depicted in Figure 3a.

In the following analysis, axial deformations of the beams and columns have been considered negligible and the two floor diaphragms have been assumed to be rigid in their own plane, while flexible in bending. Under these assumptions, the motion of the system is determined by only 6 DOFs (three for each floor), i.e., for the i-th floor, the translations u_{xi} and u_{yi} in the x and y directions and the rotation $u_{\varphi i}$ about the vertical direction (Figure 3b). Hence, the generalised displacement vector of the uncontrolled structure becomes:

$$\mathbf{X}_u(t) = \begin{bmatrix} u_{x1} & u_{y1} & u_{\varphi 1} & u_{x2} & u_{y2} & u_{\varphi 2} \end{bmatrix}^{\mathrm{T}} \tag{13}$$

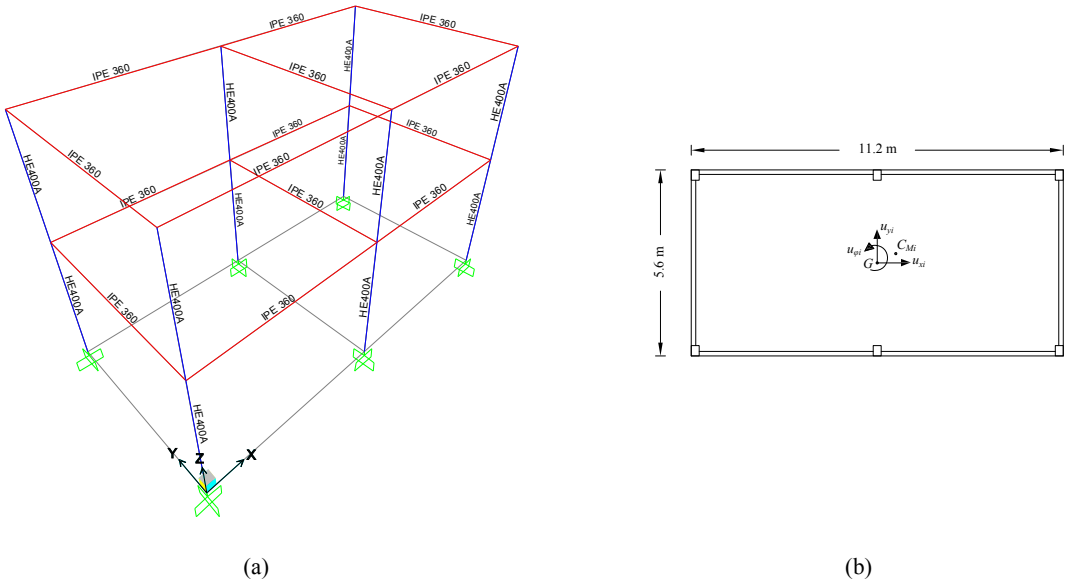

(a) (b)

Figure 3: (a) Schematic representation of the building exported from the SAP2000 software; (b) Degrees of freedom of the i-th storey.

The mass and stiffness matrices, determined by using the software SAP2000 and by utilising the static condensation technique, are:

$$\mathbf{M}_u = \begin{bmatrix} 44.42 & 0 & -19.32 & 0 & 0 & 0 \\ 0 & 44.42 & 9.66 & 0 & 0 & 0 \\ -19.32 & 9.66 & 736.59 & 0 & 0 & 0 \\ 0 & 0 & 0 & 41.42 & 0 & -19.32 \\ 0 & 0 & 0 & 0 & 41.42 & 9.66 \\ 0 & 0 & 0 & -19.32 & 9.66 & 650.49 \end{bmatrix} \cdot 10^3 \tag{14}$$

.

$$\mathbf{K}_u = \begin{bmatrix} 15.31 & 0 & 0 & -6.74 & 0 & 0 \\ 0 & 4.10 & 0 & 0 & -2.09 & 0 \\ 0 & 0 & 205.93 & 0 & 0 & -96.73 \\ -6.74 & 0 & 0 & 4.49 & 0 & 0 \\ 0 & -2.09 & 0 & 0 & 1.69 & 0 \\ 0 & 0 & -96.73 & 0 & 0 & 70.63 \end{bmatrix} \cdot 10^7 \tag{15}$$

and the damping ratio is set at 2%, which is a typical value for middle-low rise steel structures. Both mass and stiffness matrices have been computed using international system units, i.e. length are expressed in m, forces in N and masses in kg. The resulting frequencies and the percentages of the effective modal mass γ at each mode are listed in Table 1.

Mode	f_i [Hz]	ω_i [rad/s]	γ_x [%]	γ_y [%]
1	1.70	10.67	0.004	93.257
2	2.62	16.43	53.166	0.072
3	2.94	18.46	35.726	0.053
4	5.55	34.89	0.000	6.613
5	9.31	58.50	2.778	0.005
6	10.68	67.08	8.326	0.001

Table 1: Frequencies and percentage of effective modal mass for the i-th mode.

4.1 NESs design and their effectiveness

The procedure described in Section 3 has been applied to the case study structure to design a system of two independent NESs located at the top storey of the frame and acting along the x and y geometrical axes, respectively. It has been assumed that the total mass of the two NESs should not exceed 10% of the mass of the primary structure. The performance of the passive control system has been analysed considering random ground motions modelled as a Gaussian white noise process with constant PSD amplitude $S_0 = 10^{-3}$ $(\text{m/s}^2)^2/(\text{rad/s})$, selected in order to generate base acceleration peaks in the order of 0.25 g (typical range of ground accelerations in civil engineering applications). To assess the mutual effects of the two NESs, the analysis has been performed considering various epicentral directions of the ground motion.

Based on the results of the preliminary modal analysis on the uncontrolled structure (see Table 1):

- the NES acting in the y direction has been designed by applying Eqs. (11) and (12) to a dummy SDOF structure with natural frequency equal to the 1st modal frequency of the building ($\omega_1 = 10.67$ rad/s);
- the NES in the x direction has been designed with respect to a dummy SDOF structure having natural frequency equal to the 2nd modal frequency ($\omega_2 = 16.43$ rad/s);

In both cases, the damping ratio of the equivalent SDOF has been set to 2% (as for the main building) and the NES masses have been calculated as 5% of the effective modal masses for the

NES along x-axis			NES along y-axis		
$m_{NES,x}$ [kg]	$k_{NES,x}$ [N/m^3]	$c_{NES,x}$ [Ns/m]	$m_{NES,y}$ [kg]	$k_{NES,y}$ [N/m^3]	$c_{NES,y}$ [Ns/m]
$3.28 \cdot 10^3$	$10^{9.72}$	$1.02 \cdot 10^4$	$4.00 \cdot 10^3$	$10^{9.03}$	$1.16 \cdot 10^4$

Table 2: NES parameters for the two NESs obtained using the proposed method.

first two modes, respectively, i.e.:

$$m_{NES,y} = 0.05\, m_{1e,y} = 0.05\, \gamma_y^{(1)} \boldsymbol{\tau}_y^T \mathbf{M}_u \boldsymbol{\tau}_y \qquad (16)$$
$$m_{NES,x} = 0.05\, m_{1e,x} = 0.05\, \gamma_x^{(2)} \boldsymbol{\tau}_x^T \mathbf{M}_u \boldsymbol{\tau}_x$$

In Eq.(16), $\boldsymbol{\tau}_x$ and $\boldsymbol{\tau}_y$ are the influence vectors for the cases of ground motion acting in the x and y directions respectively; $\gamma_y^{(1)}$ and $\gamma_x^{(2)}$ are the percentages of effective modal masses at the fundamental modes in y-direction and in x-direction, respectively; $\mathbf{M}_u$ is the mass matrix of the primary structure, as shown in Eq. (14). The resulting parameters of the two NESs are reported in Table 2. The equations of motion of the combined system are given by Eqs. (2) and (5), considering $p = 2$, and $\mathbf{L}$ and $\boldsymbol{\tau}$ as:

$$\mathbf{L} = \begin{bmatrix} 0 & 0 \\ 0 & 0 \\ 0 & 0 \\ 1 & 0 \\ 0 & 1 \\ 0 & 0 \\ -1 & 0 \\ 0 & -1 \end{bmatrix}; \qquad \boldsymbol{\tau} = \begin{bmatrix} \cos\theta \\ \sin\theta \\ 0 \\ \cos\theta \\ \sin\theta \\ 0 \\ \cos\theta \\ \sin\theta \end{bmatrix}. \qquad (17)$$

The effects of the NESs have been investigated varying the epicentral direction of the ground motion, θ, ranging from 0° (i.e. x-direction) to 90° (i.e. y-direction) with step of 15°. Results of the analysis are presented in terms of statistics of the response, and energy dissipated by the primary structure and by the passive control system.

The first comparison between the uncontrolled and controlled configurations is presented in terms of variance of the magnitude of the inter-storey displacements, defined as:

$$d_{1,U} = \sqrt{u_{x1,U}^2 + u_{y1,U}^2} \qquad d_{2,U} = \sqrt{(u_{x2,U} - u_{x1,U})^2 + (u_{y2,U} - u_{y1,U})^2} \qquad (18)$$

$$d_{1,C} = \sqrt{u_{x1,C}^2 + u_{y1,C}^2} \qquad d_{2,C} = \sqrt{(u_{x2,C} - u_{x1,C})^2 + (u_{y2,C} - u_{y1,C})^2} \qquad (19)$$

where the subscripts U and C stand for uncontrolled and controlled configurations, respectively. Numerical results have been obtained by performing MCSs using, for each analysis, 10,000 base acceleration time histories, 20 s long, sampled with a time step of 0.01 s. The nonlinear equations of motion have been integrated by the 4th-order Runge-Kutta method.

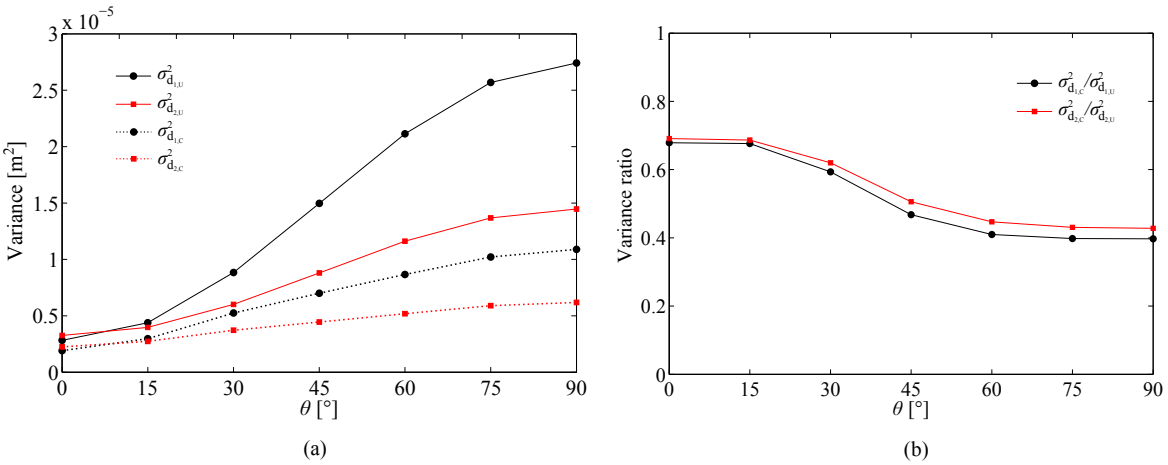

Figure 4: (a) Variance of inter-storey displacements of the structure in its controlled and uncontrolled configurations versus the incidence angle of the ground motion; (b) Ratio of the variances of inter-storey displacements of the structure between the controlled and uncontrolled configurations for each floor versus the incidence angle of the ground motion.

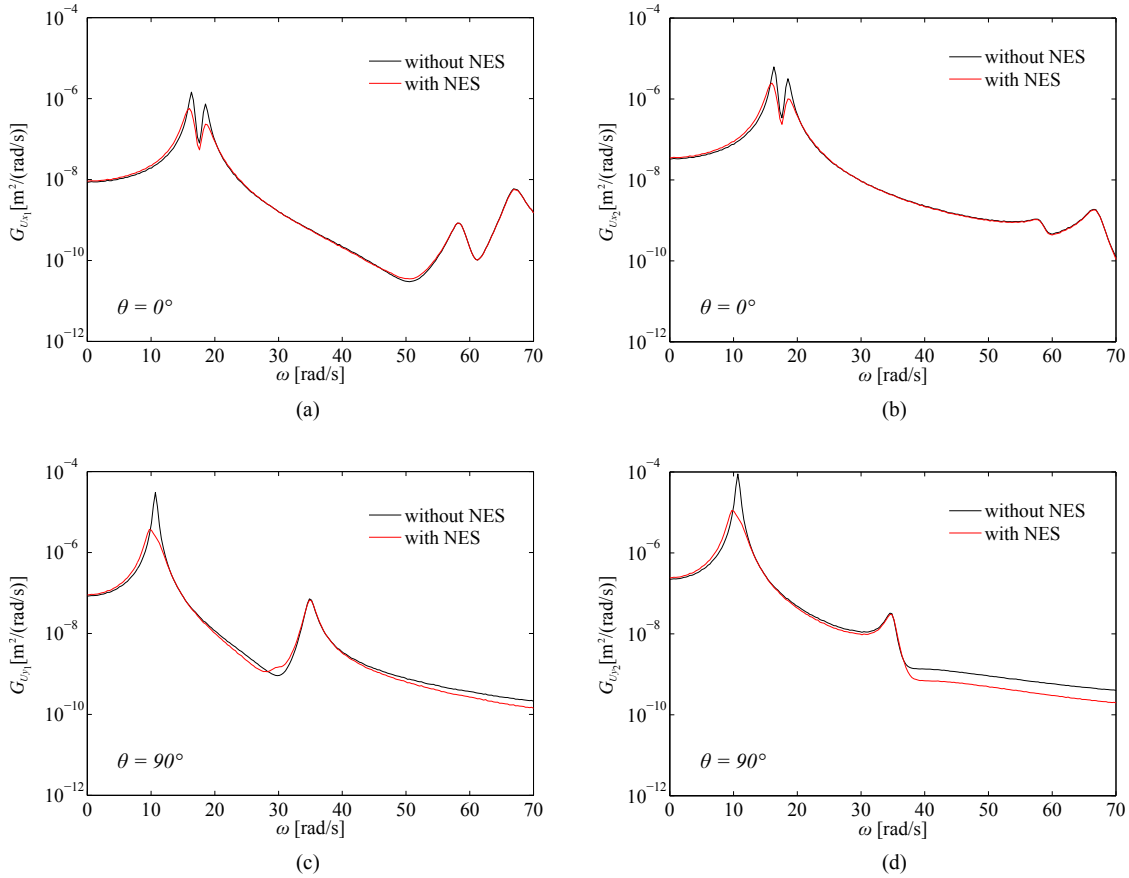

Figure 5: Comparison between the uncontrolled and controlled configurations of the system in terms of: (a)-(b) PSD of the displacements of the first and second floor, respectively, in x direction for $\theta = 0°$; (c)-(d) PSD of the displacements of the first and second floor, respectively, in y direction for $\theta = 90°$.

Figure 4 shows the outcome of the numerical analysis varying θ. The variance of the struc-

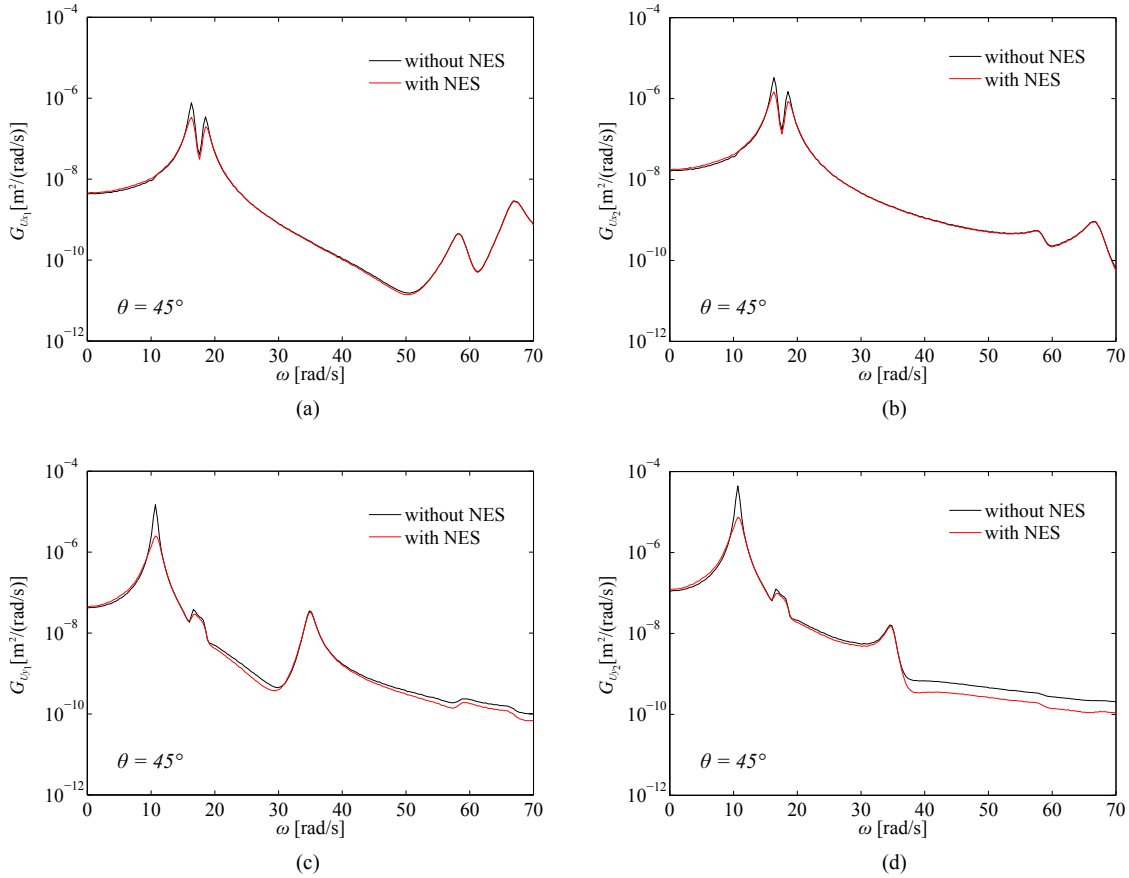

Figure 6: Comparison between the uncontrolled and controlled configurations of the system in terms of: (a)-(b) PSD of the displacements of the first and second floor, respectively, in x direction for $\theta = 45°$; (c)-(d) PSD of the displacements of the first and second floor, respectively, in y direction for $\theta = 45°$.

tural displacements increases with θ for both controlled and uncontrolled configurations. However, in terms of percentage reduction of the response, the NES effectiveness is actually larger for higher values of θ, with a maximum reduction of the variance of the displacements of around 60% (Figure 4b).

For a better understanding of the actual effects of the two NESs, the response of the uncontrolled and controlled configurations are also compared in terms of PSDs of the displacements, in the x and y directions, of the two storeys of the examined building. For $\theta = 0°$ and $\theta = 90°$, the PSDs of the displacements in the x and y directions, respectively, are depicted in Figure 5. Additionally, Figure 6 shows the PSDs of both displacements in x and y directions, for both storeys, when $\theta = 45°$. While the effects of the NES is prevalent on the first two modes of the structure (i.e. on the modes considered for the design of the NES parameters), the whole passive control system also affects the 3rd mode.

Finally, the NES performance has been analysed in terms of total dissipated energy in the two configurations (uncontrolled and controlled), obtained as the average of the energy dissipated over the 10,000 samples. In particular, Figure 7 shows:

- the energy dissipated by the structure in the uncontrolled configuration, $E_{d,U}$;
- the energy dissipated in the controlled configuration by (i) the primary structure, $E_{d,C}$; (ii) the NES in the x direction, $E_{d,Nx}$; (iii) the NES in the y direction, $E_{d,Ny}$;

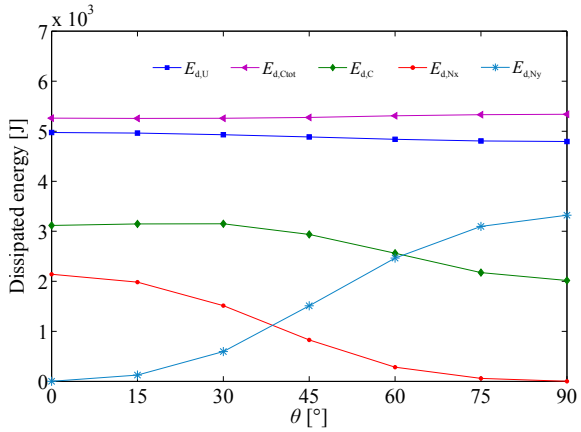

Figure 7: Total dissipated energy in the uncontrolled and controlled configurations versus the incidence angle of the ground motion.

- the total energy dissipated in the controlled configuration, $E_{d,Ctot} = E_{d,C} + E_{d,Nx} + E_{d,Ny}$.

The contribute of energy dissipated by the system of the two NESs varies from 40% to 62% of the total dissipated energy, depending on the direction of the ground motion. The energy dissipated by the NESs increases with θ changing from $0°$ to $90°$. Positively, the variance of the displacements of the uncontrolled structure increases with θ, therefore the two nonlinear devices dissipate a higher percentage of energy when the system is more affected by the external excitation, which is the most desirable behaviour for the passive control system. This also confirms the results shown in Figure 4b.

5 CONCLUSIONS

In this paper, a simplified procedure for evaluating the NES parameters to mitigate the dynamic response of a MDOF structure subject to white noise base excitations has been proposed and validated. The NES design can be carried out by considering dummy SDOF structures whose dynamic parameters depend on the fundamental modes of the structure. Then, each NES is optimised with respect to one of the dummy structures by using the empirical formulae or, alternatively, the design charts proposed in [22].

The applicability of this procedure to MDOF structures has been demonstrated through a case study consisting of a low-rise building controlled by two NESs and excited by white noise base processes. The reference structure is a two-bay and two-storey steel frame supporting concrete slabs, having eccentric centre of mass.

It has been shown that the proposed procedure allows to quickly design the two NESs so that they both dissipate a significant percentage of energy in the main system. Naturally, the effect of each NES depends on the direction of the ground motion. However, it has been observed that the effectiveness of the whole passive control system increases with the raise of the frame displacements. This is the most desirable behaviour, and confirms the validity of the proposed procedure. Further research is necessary to validate the proposed approach against a full numerical optimisation of the NES parameters, and to establish the most effective position and direction of action for each NES to achieve the highest performance.

REFERENCES

[1] G.W. Housner, L.A. Bergman, T.K. Caughey, A.G. Chassiakos, R.O. Claus, S.F. Masri, R.E. Skelton, T.T. Soong, B.F. Spencer, J.T.P. Yao, Structural Control : Past, present, and future. *Journal of Engineering Mechanics*, **123**(9), 897–971, 1997.

[2] T. Asami, O. Nishihara, A.M. Baz, Analytical solutions to H_∞ and H_2 optimization of dynamic vibration absorbers attached to damped linear systems. *Journal of Vibration and Acoustics*, **124**(2), 284–295, 2002.

[3] A. Ghosh, B. Basu, A closed-form optimal tuning criterion for TMD in damped structures. *Structural Control and Health Monitoring*, **14**(4), 681–692, 2007.

[4] A. Di Matteo, F. Lo Iacono, G. Navarra, A. Pirrotta, Optimal tuning of tuned liquid column damper systems in random vibration by means of an approximate formulation. *Meccanica*, **50**, 795–808, 2015. doi:10.1007/s11012-014-0051-6.

[5] A. Di Matteo, F. Lo Iacono, G. Navarra, A. Pirrotta, Innovative modeling of tuned liquid column damper motion. *Communications in Nonlinear Science and Numerical Simulation*, **23**(1–3), 229–244, 2015. doi:10.1016/j.cnsns.2014.11.005.

[6] O. Gendelman, L.I. Manevitch, A.F. Vakakis, R. M'Closkey, Energy pumping in nonlinear mechanical oscillators: Part I - Dynamics of the underlying hamiltonian systems. *Journal of Applied Mechanics*, **68**(1), 34–41, 2001.

[7] A.F. Vakakis, O.V. Gendelman, Energy pumping in nonlinear mechanical oscillators: Part II - Resonance capture. *Journal of Applied Mechanics*, **68**(1), 42–48, 2001.

[8] O.V. Gendelman, Transition of energy to a nonlinear localized mode in a highly asymmetric system of two oscillators. *Nonlinear Dynamics*, **25**, 237–53, 2001.

[9] G. Kerschen, Y.S. Lee , A.F. Vakakis, D.M. McFarland , L.A. Bergman, Irreversible passive energy transfer in coupled oscillators with essential nonlinearity. *SIAM Journal on Applied Mathematics*, **66**(2), 648–679, 2006.

[10] Y.S. Lee, G. Kerschen, A.F. Vakakis, P. Panagopoulos, L.A. Bergman, D.M. McFarland, Complicated dynamics of a linear oscillator with a light, essentially nonlinear attachment. *Physica D: Nonlinear Phenomena*, **204**, 41–69, 2005.

[11] F. Nucera, A.F. Vakakis, D.M. McFarland, L.A. Bergman, G. Kerschen, Targeted energy transfers in vibro-impact oscillators for seismic mitigation. *Nonlinear Dynamics*, **50**(3), 651–677, 2007.

[12] A.F. Vakakis, O.V. Gendelman, L.A. Bergman, D.M. McFarland, G. Kerschen, Y.S. Lee, *Nonlinear targeted energy transfer in mechanical and structural systems*. Springer Netherlands, 2009.

[13] D.M. McFarland, L.A. Bergman, A.F. Vakakis, Experimental study of non-linear energy pumping occurring at a single fast frequency. *International Journal of Non-Linear Mechanics*, **40**(6), 891–899, 2005.

[14] G. Kerschen, D.M. McFarland, J.J. Kowtko, Y.S. Lee, L.A. Bergman, A.F. Vakakis, Experimental demonstration of transient resonance capture in a system of two coupled oscillators with essential stiffness nonlinearity. *Journal of Sound and Vibration*, **299**(4–5), 822–38, 2007.

[15] E. Gourdon, N.A. Alexander, C.A. Taylor , C.H. Lamarque, S. Pernot, Nonlinear energy pumping under transient forcing with strongly nonlinear coupling: theoretical and experimental results. *Journal of Sound and Vibration*, **300**(3–5), 522–51, 2007.

[16] F. Nucera, F. Lo Iacono, D.M. McFarland, L.A. Bergman, A.F. Vakakis, Application of broadband nonlinear targeted energy transfers for seismic mitigation of a shear frame: Experimental results. *Journal of Sound and Vibration*, **313**(1–2), 57–76, 2008. doi:10.1016/j.jsv.2007.11.018.

[17] N.E. Wierschem, D.D. Quinn, S.A. Hubbard, M.A. Al-Shudeifat, D.M. McFarland, J. Luo, L.A. Fahnestock, B.F. Spencer, A.F. Vakakis, L.A. Bergman, Passive damping enhancement of a two-degree-of-freedom system through a strongly nonlinear two-degree-of-freedom attachment. *Journal of Sound and Vibration*, **331**(25), 5393–5407, 2012.

[18] J. Luo, N.E. Wierschem, S.A. Hubbard, L.A. Fahnestock, D.D. Quinn, D.M. McFarland, B.F. Spencer, A.F. Vakakis, L.A. Bergman, Large-scale experimental evaluation and numerical simulation of a system of nonlinear energy sinks for seismic mitigation. *Engineering Structures*, **77**, 34–48, 2014.

[19] Y. Starosvetsky, O.V. Gendelman, Attractors of harmonically forced linear oscillator with attached nonlinear energy sink. II: Optimization of a nonlinear vibration absorber. *Nonlinear Dynamics* , **51**(47), 47–57, 2008.

[20] B. Vaurigaud, A. Ture Savadkoohi, C.H. Lamarque, Targeted energy transfer with parallel nonlinear energy sinks. Part I: Design theory and numerical results. *Nonlinear Dynamics*, **66**(4), 763–780, 2011.

[21] T.A. Nguyen, S. Pernot, Design criteria for optimally tuned nonlinear energy sinks – part 1: transient regime. *Nonlinear Dynamics*, **69**(1–2), 1–19, 2012.

[22] M. Oliva, G. Barone, G. Navarra, Optimal design of Nonlinear Energy Sinks for SDOF structures subjected to white noise base excitations. *Engineering Structures* **145**, 135–152, 2017. doi:10.1016/j.engstruct.2017.03.027.